CHAPTER 10.B

Analysis of alternative conformations of the Aβ(1−40) amyloid protein

Dawid Dułak[1], Małgorzata Gadzała[2], Mateusz Banach[3], Irena Roterman[3]

[1]Department of Biophysics, Faculty of Physics, Astronomy and Applied Computer Sciencee Jagiellonian University, Krakow, Poland
[2]Cyfronet AGH Academic Computer Centre CYFRONET - University of Science and Technology in Cracow, Kraków, Poland; Currently - Schibsted Tech Polska Sp. z o. o., Kraków, Poland
[3]Department of Bioinformatics and Telemedicine, Jagiellonian University−Medical College, Krakow, Poland

Contents

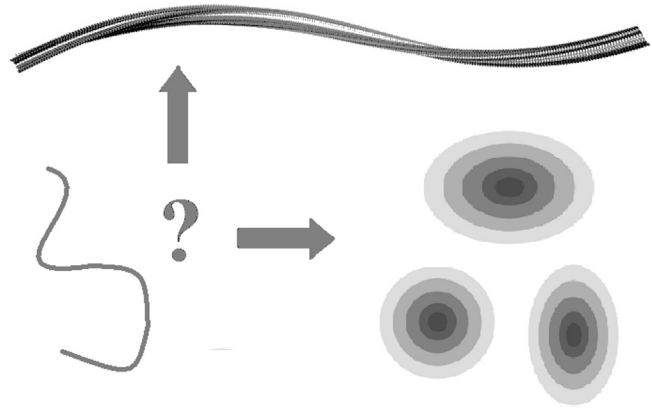

From Globular Proteins to Amyloids
ISBN: 978-0-08-102981-7
https://doi.org/10.1016/B978-0-08-102981-7.00017-8

Making decision by the folding polypeptide: amyloid ? or globular ?

Alternative structural forms of polypeptide Aβ(1−40) polypeptide which includes the Osaka mutation

The amyloid structures like for example Aβ(1−40) [1] become available due to new technique ssNMR [2]. A polypeptide corresponding to the Aβ(1−40) sequence with the so-called Osaka mutation was subjected to an *in silico* experiment. Specialized folding software was used to generate five different folds per software package, in accordance with the rules of the CASP challenge. The experiment provided structures which could be regarded as alternative with respect to the experimentally observed conformation (PDB ID: 2MVX [1]). This, in turn, facilitated comparative analysis aimed at identifying fragments which support or deviate from the expected monocentric distribution of hydrophobicity. The presence of a centralized hydrophobic core provides the protein with solubility and thereby prevents unchecked complexation (potentially producing an amyloid). In addition to the above, the folding process was simulated in the presence of an external force field (FOD model) which mimics the active participation of aqueous solvent in folding process. The resulting structures provide evidence that − under the appropriate conditions − the Aβ(1−40) polypeptide may adopt a globular conformation, and suggest that the environment plays a critical role in this process.

In an attempt to identify the causes of amyloid transformation of sequences which include the Aβ(1−40) fragment, we have performed an *in silico* experiment to identify possible conformational preferences of this polypeptide. The experiment involved folding simulation tools currently regarded as the most accurate: I-Tasser [3−6] and Robetta [7−9] - two of the highest-scoring CASP challenge entrants [10]. Both are capable of predicting the conformation of chains with a given sequence, and each produces five distinct candidate structures, referred to as models. We subjected these models to comparative analysis set against the backdrop of the experimentally observed structure (obtained using ssNMR). In addition to the above, the input polypeptide was also subjected to simulations based on the fuzzy oil drop (FOD) model, which asserts the presence of an external force field representing the aqueous solvent and treated as a continuum − unlike other algorithms where the solvent is modeled as a collection of individual molecules [11,12]. In FOD, the solvent is mathematically

represented by a 3D Gaussian form, directing hydrophobic residues toward the center of the protein body while exposing hydrophilic residues on its surface. The resulting set of models enhances our ability to perform comparative analysis of amyloid structures with the outcomes of *in silico* folding simulations.

All computations using FOD were performed at the Academic Computing Center CYFRONET AGH using resources provided by the PL-Grid infrastructure.

The resulting set of 20 models (FOD: 5, I-Tasser: 5, Robetta: 10) is the subject of the presented analysis. Each model will be compared to the experimentally determined target structure – both in the context of the superfibril and as an individual chain.

In order to carry out comparative analysis, we begin by computing fuzzy oil drop coefficients for all models. This includes values of RD (relative distance – as defined by Kullback-Leibler divergence entropy) in two distinct reference models: T-O-R and T-O-H respectively [13].

The FOD model, presented in Chapter 1, suggests that the value of RD(T-O-H) is particularly important. As proposed in Refs. [14,15], which deals with the structure of the tau amyloid, amyloid seeds may be identified by looking for high values of RD (T-O-R as well as T-O-H), along with negative values of HvT and TvO and strongly positive values of HvO. These specific conditions indicate that the given fragment opposes the theoretical distribution of hydrophobicity, and is dominated by the intrinsic properties of its residues.

Values of RD and correlation coefficients may be calculated for the entire protein (polypeptide), but also for selected fragments. In the latter case, the process tells us whether the given fragment contributes to the creation of a hydrophobic core or opposes it

The structure listed in PDB under ID 2MVX consists of two protofibrils exhibiting C2 symmetry. Each protofibril resembles a flattened "C", and contacts the opposing protofibril at both tips, while exposing its backside to the environment. In order to determine the FOD status of the superfibril we compute its T and O distributions (Figs. 10.B.1 and 10.B.2). As shown in Fig. 10.B.1, these distributions are a poor match for each other. In particular, no concentration of hydrophobicity can be

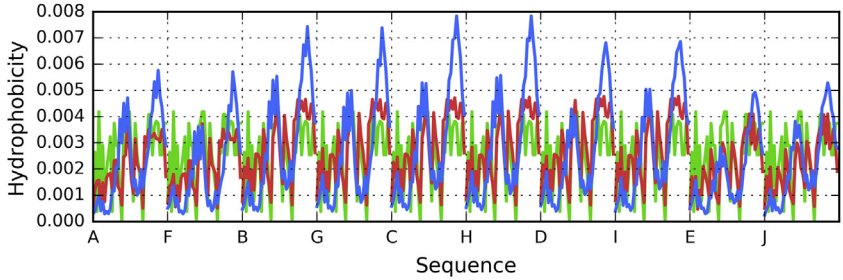

Fig. 10.B.1 Theoretical (T, blue), observed (O, red) and intrinsic (H, green) hydrophobicity distribution profiles for Aβ(1−40) (2MVX) superfibril.

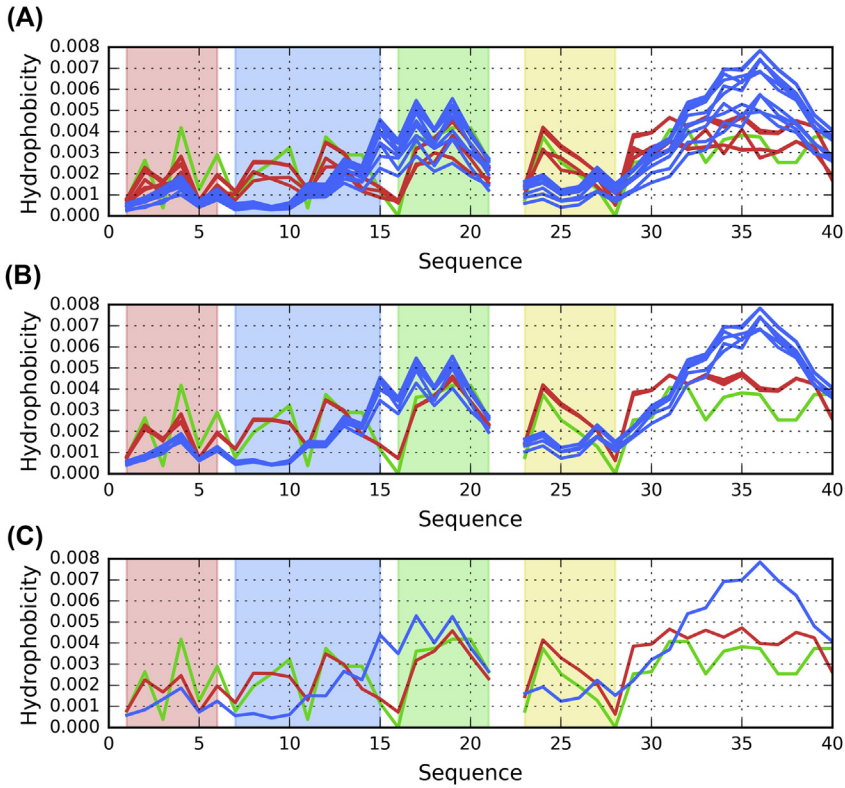

Fig. 10.B.2 Theoretical (T, blue), observed (O, red) and intrinsic (H, green) hydrophobicity distribution profiles for Aβ(1−40) (2MVX). (A) superfibril (chains A − J). (B) central part of the superfibril (following elimination of the outlying chains A, E, F and J). (C) individual (central) chain C treated as part of superfibril. Colored backgrounds highlight fragments analyzed in this study: red − 1-6, blue − 7-15, green − 16-21, yellow − 23-28. There is no residue number 22 in the sequence, however there is no gap in the chains within the PDB structure.

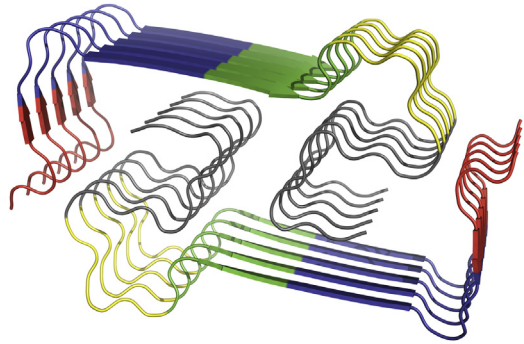

Fig. 10.B.3 3D presentation of Aβ(1−40) (2MVX) with fragments analyzed in this study highlighted by different colors: red − 1−6, blue − 7−15, green − 16−21, yellow − 23−28. Rest of each chain (29−40) is gray.

observed in the central part of the structure; instead, hydrophobicity is evenly distributed along the fibril's main axis. This type of distribution, where bands of high and low hydrophobicity propagate in an alternating fashion, resulting in a sinusoid pattern, is typical for amyloids. It follows from the repetitive nature of the input chain, as well as from conformational symmetries between each set of fragments making up the fibril (Fig. 10.B.3).

In the presented case, FOD parameters adopt the following values: RD (T-O-R) = 0.590; RD (T-O-H) = 0.592; HvT = 0.438; TvO = 0.673; HvO = 0.727. These results suggest that the structure as a whole does not contain a prominent hydrophobic core, and furthermore that the superfibril represents a consensus between the tendency to generate such a core and the intrinsic properties of each participating residue.

In contrast to Fig. 10.B.2A, profiles shown in Fig. 10.B.2B represents the distribution of hydrophobicity taking the entire superfibril as the structural unit for 3D Gauss construction.

Theoretical distribution, plotted in Fig. 10.B.2A and Fig. 10.B.2B, reveal the expected concentration of hydrophobicity in the central section of the fibril. The variability observed in Fig. 10.B.2B is due to the presence of edge chains, which lack an outlying neighbor and therefore exhibit slightly lower hydrophobicity than their centrally located counterparts (Fig. 10.B.2B). In contrast, the intrinsic distribution (H) distribution follows a sinusoidal pattern since all participating chains share identical sequences. The observed distribution (O) is also sinusoidal, consisting of alternating

minima and maxima. Fig. 10.B.2B also reveals the high similarity of repeating patterns for O and H.

Fig. 10.B.2B visualizes the theoretical and observed distributions for the central chain treated as part of superfibril. Comparing both plots reveals significant differences at positions 7–15, 16–21, 22–27 and 23–28. Rather than being limited to modest deviations, these differences point to an entirely different structural pattern, counteracting the tendency to form a shared hydrophobic core.

Similar discordance is observed when calculating hydrophobicity profiles for chain C treated as part of protofibril (centrally placed chain C – Fig. 10.B.2C). The abovementioned discordant fragments will be subjected to further analysis, comparing them with the structural properties of *in silico* models.

Plotting a 3D Gaussian for the entire complex (superfibril) also enables us to determine the status of interface fragments, i.e. those residues which remain in contact with adjacent protofibrils. The status of the interface (residues satisfying the distance criterion according to PDBsum [16]: 3, 4,15, 28, 29, 30, 37–40) expressed by FOD parameters is given by the following RD values: 0.432 and 0.387 (T-O-R and T-O-H respectively), while correlation coefficients are 0.378, 0.672 and 0.658 (HvT, TvO and HvO respectively). These values indicate good alignment between the observed distribution of hydrophobicity and the distribution predicted by the fuzzy oil drop model. Notably, TvO and HvO lead us to conclude that O is similarly aligned with T and H. We may therefore speculate that while each protofibril is dominated by the intrinsic hydrophobicity of its component residues, the entire complex (superfibril) forms as a result of interactions between protofibrils which acknowledge the presence of the aqueous environment.

Comparative analysis of protein structures generated using folding simulation software

Similarly to the analysis of the Aβ(15–40) (PDB ID: 2MPZ) [15], we will conduct a comparative study by seeking fragment of the chain whose properties suggest that they may act as amyloid seeds. In other words, the fragments of interest need to be characterized by the following: high value of HvO and negative values of both HvT and TvO. A negative correlation coefficient suggests that the given fragment not only deviates from the

reference distribution, but in fact may be regarded as a polar opposite thereof. When such values are accompanied by high RD (above 0.5), we may suspect that the conformation of the given fragment is determined by the intrinsic hydrophobicity of its residues.

As it was discussed formerly [15], to search the origin of the amyloidosis tendency of the polypeptide, the best programs predicting the structure for given amino acid sequence were used to construct alternative structural forms for this polypeptide: I-TASSER [3−5] and ROSETTA [6−9]. These two programs delived 5 alternative structural forms for given sequence (following the CASP project rule [10]). As was said earlier − Robetta delivered 10 models in this case. Additionally, the folding was performed using fuzzy oil drop model (Chapter 2). The FOD model based folding simulation delivers the structures formed by the active participation of water environment. In this study, structures belonging to the output generated by I-Tasser and Robetta are marked by letters I and R respectively. Names of structures generated by FOD start with F. Number following these IDs distinguish the individual models.

Table 10.B.1 lists the FOD coefficients (both values of RD as well as all three correlation coefficients − HvT, TvO and HvO) for each fragment under consideration: 1−6, 7−15, 16−21, 23−28. The study set consists of models obtained using Robetta (R1…R10), I-Tasser (I1…I5) and FOD-based simulations (F1…F5). It also contains results for a representative of native structure of Aβ(1−40) − chain C from 2MVX (as part of superfibril and as an individual unit).

The presented results suggest that structures labeled F1, F2, F3 as well as R1, R2, R3 and R4 are all consistent with the theoretical distribution, implying that the chain is capable of adopting a globular conformation. Table 10.B.1 also highlights forms which exhibit amyloid-like properties − evidenced by negative values of both HvT and TvO, a strongly positive value of HvO, and high values of both RD (T-O-R and T-O-H). All such structures are underscored in the table.

In most cases, however, the RD value for the T-O-H reference model is not particularly high. This may be explained by observing that we are dealing with standalone individual chains − in contrast to chains analyzed as part of an amyloid fibril. Under such conditions the dominant role of intrinsic hydrophobicity is not as evident as could be expected taking into account the structural forms obtained by FOD and Robetta: F1, F2, F3 as well as R1, R2, R3 and R4.

When summarizing the results presented in Table 10.B.1 (see Table 10.B.2 for a compact presentation), it is worth noting that the

Table.1 Fuzzy oil drop parameters for simulated model structures of 2MVX / Aβ(1-40) and their fragments (as denoted by the leftmost column), sorted in order of increasing RD(T-O-R) values for the whole chain. Columns "M" contains model names (which also designate methods used to obtain them): F1…F5 — FOD, I1...I5 — I-Tasser, R1...R10 — Robetta. "CC" stands for chain C from experimentally determined structure of 2MVX treated as part of the complex, while CS — as a standalone structure.

		RD		Correlation Coefficient				RD		Correlation Coefficient				RD		Correlation Coefficient		
FRAGMENT	**M**	**T-O-R**	**T-O-H**	**HvT**	**TvO**	**HvO**	**M**	**T-O-R**	**T-O-H**	**HvT**	**TvO**	**HvO**	**M**	**T-O-R**	**T-O-H**	**HvT**	**TvO**	**HvO**
1-40	F1	0.250	0.216	0.251	0.819	0.378	F2	0.266	0.235	0.246	0.815	0.372	F3	0.279	0.224	0.164	0.799	0.358
1—6		0.448	0.154	-0.319	0.543	-0.329		0.775	0.289	0.831	-0.506	-0.187		0.675	0.329	0.308	-0.041	0.061
07—15		0.264	0.201	0.428	0.831	0.403		0.389	0.310	0.148	0.561	0.359		0.392	0.306	0.365	0.557	0.372
16—21		0.306	0.195	0.188	0.820	0.613		0.448	0.399	0.005	0.552	0.702		0.342	0.292	0.077	0.802	0.593
23—28		0.243	0.234	0.430	0.907	0.676		0.243	0.150	0.166	0.804	0.594		0.321	0.110	-0.214	0.757	0.450
29—40		0.396	0.211	-0.273	0.727	-0.555		0.233	0.130	-0.322	0.846	-0.538		0.245	0.137	-0.417	0.829	-0.538
11—19		0.287	0.196	0.231	0.778	0.652		0.399	0.324	0.115	0.610	0.666		0.436	0.357	0.154	0.576	0.641
1—40	R1	0.434	0.375	0.502	0.578	0.704	R2	0.458	0.438	0.501	0.564	0.694	R3	0.465	0.457	0.459	0.531	0.703
1—6		0.356	0.328	0.674	0.805	0.822		0.203	0.206	0.632	0.892	0.721		0.168	0.139	0.788	0.904	0.880
07—15		0.486	0.874	0.444	0.535	0.945		0.539	0.488	0.215	0.341	0.617		0.717	0.450	-0.121	0.231	0.867
16—21		0.200	0.065	0.829	0.894	0.870		0.240	0.254	0.827	0.855	0.831		0.196	0.282	0.814	0.918	0.836
23—28		0.356	0.058	0.015	0.727	0.527		0.639	0.133	0.072	0.228	0.804		0.604	0.113	0.018	0.253	0.800
29—40		0.482	0.382	0.230	0.781	0.085		0.725	0.573	0.287	0.609	-0.005		0.747	0.595	0.287	0.619	0.033
11—19		0.404	0.277	0.650	0.697	0.929		0.212	0.281	0.786	0.894	0.817		0.139	0.225	0.782	0.957	0.850
1—40	R4	0.465	0.365	0.414	0.565	0.755	R5	0.508	0.506	0.411	0.465	0.791	R6	0.509	0.500	0.555	0.544	0.780
1—6		0.229	0.425	0.832	0.864	0.985		0.378	0.658	0.643	0.656	0.965		0.297	0.478	0.832	0.775	0.958
07—15		0.356	0.349	0.510	0.719	0.739		0.330	0.423	0.505	0.770	0.813		0.493	0.533	0.489	0.595	0.797
16—21		0.112	0.047	0.759	0.934	0.872		0.580	0.139	0.050	0.131	0.748		0.354	0.222	0.852	0.559	0.747
23—28		0.616	0.121	-0.335	0.283	0.479		0.396	0.547	0.340	0.671	0.920		0.592	0.260	0.031	0.251	0.862
29—40		0.770	0.568	-0.050	0.325	-0.119		0.753	0.723	0.206	0.371	0.376		0.749	0.695	0.192	0.267	0.273
11—19		0.117	0.097	0.895	0.975	0.877		0.331	0.159	0.457	0.726	0.869		0.187	0.154	0.856	0.821	0.837
1—40	R7	0.519	0.434	0.412	0.436	0.721	R8	0.532	0.427	0.370	0.515	0.681	I1	0.602	0.409	0.132	0.332	0.516
1—6		0.218	0.101	0.824	0.909	0.804		0.330	0.125	0.235	0.856	0.290		0.421	0.243	0.666	0.472	0.275
07—15		0.618	0.515	-0.075	0.229	0.869		0.746	0.668	-0.103	-0.154	0.913		0.806	0.348	-0.412	0.049	-0.475

16−21		0.255	0.132	0.746	0.815	0.771		0.265	0.155	0.833	0.803	0.840		0.652	0.385	−0.350	−0.591	0.859
23−28		0.422	0.078	0.231	0.509	0.857		0.727	0.190	−0.119	0.010	0.806		0.814	0.253	−0.866	−0.609	0.291
29−40		0.790	0.684	0.231	0.345	0.149		0.767	0.687	0.289	0.323	0.145		0.792	0.744	0.366	0.521	0.287
11−19		0.136	0.110	0.724	0.937	0.828		0.145	0.120	0.762	0.923	0.824		0.492	0.222	−0.173	0.363	0.526
1−40	CC	0.608	0.620	0.459	0.665	0.784	I2	0.623	0.508	0.147	0.218	0.540	F4	0.629	0.368	−0.157	0.312	0.238
1−6		0.332	0.207	0.621	0.739	0.770		0.352	0.157	−0.317	0.680	0.322		0.506	0.111	−0.406	0.593	−0.283
07−15		0.857	0.857	−0.113	−0.198	0.850		0.762	0.641	0.222	−0.250	0.433		0.623	0.499	0.152	0.727	0.531
16−21		0.407	0.282	0.485	0.622	0.946		0.677	0.602	−0.593	−0.905	0.792		0.581	0.358	−0.020	0.196	0.726
23−28		0.533	0.461	0.065	0.039	0.995		0.648	0.108	−0.643	−0.153	0.403		0.680	0.293	−0.958	−0.342	0.417
29−40		0.853	0.648	0.157	0.301	−0.005		0.758	0.617	0.140	0.344	−0.285		0.548	0.386	−0.260	0.607	−0.672
11−19		0.565	0.484	0.285	0.348	0.929		0.564	0.482	−0.110	−0.182	0.776		0.371	0.215	0.156	0.631	0.697
1−40	F5	0.631	0.433	−0.122	0.350	0.285	I3	0.634	0.372	0.134	0.401	0.552	CS	0.636	0.562	0.295	0.363	0.616
1−6		0.466	0.329	−0.101	0.530	0.251		0.576	0.325	−0.162	0.185	0.622		0.682	0.370	0.747	0.025	0.233
07−15		0.756	0.454	0.358	0.356	0.295		0.859	0.600	−0.325	−0.283	0.173		0.864	0.783	−0.062	−0.405	0.606
16−21		0.542	0.324	−0.767	0.145	0.397		0.499	0.162	0.330	0.492	0.876		0.456	0.171	0.199	0.407	0.844
23−28		0.821	0.443	−0.920	−0.903	0.754		0.790	0.122	−0.797	−0.148	0.015		0.421	0.230	0.494	0.508	0.994
29−40		0.659	0.506	0.040	0.587	−0.514		0.884	0.723	0.204	0.626	−0.139		0.797	0.690	0.159	0.611	−0.022
11−19		0.473	0.217	−0.144	0.618	0.211		0.407	0.177	0.169	0.624	0.627		0.568	0.362	0.213	0.258	0.809
1−40	I4	0.642	0.459	0.277	0.333	0.491	R9	0.650	0.601	0.372	0.413	0.757	I5	0.702	0.521	0.266	0.208	0.533
1−6		0.419	0.531	0.805	0.532	0.847		0.602	0.555	0.357	−0.157	0.684		0.740	0.566	0.403	0.381	0.917
07−15		0.886	0.502	−0.099	−0.447	0.200		0.685	0.892	0.317	0.155	0.909		0.893	0.673	−0.079	−0.836	0.183
16−21		0.722	0.467	0.124	−0.460	0.615		0.723	0.297	−0.393	−0.394	0.798		0.662	0.510	−0.006	−0.459	0.693
23−28		0.808	0.299	−0.760	−0.454	0.665		0.459	0.312	0.275	0.440	0.914		0.837	0.222	−0.844	−0.452	0.143
29−40		0.502	0.357	0.185	0.618	−0.392		0.737	0.644	0.119	0.454	0.169		0.728	0.462	0.473	0.410	−0.504
11−19		0.446	0.231	0.254	0.444	0.673		0.509	0.320	0.087	0.217	0.827		0.542	0.340	0.038	0.199	0.711
1−40	R10	0.718	0.612	0.142	0.025	0.680												
1−6		0.669	0.467	0.781	0.062	0.615												
07−15		0.782	0.630	−0.070	−0.390	0.701												
16−21		0.527	0.135	0.027	0.129	0.802												
23−28		0.269	0.080	0.676	0.810	0.965												
29−40		0.724	0.822	0.587	0.422	0.693												
11−19		0.515	0.160	−0.012	0.244	0.886												

Table 10.B.2 Status of suspected amyloid seeds in simulated model structures of Aβ(1−40), compared with experimental observations (2MVX structure). Numbers in the table correspond to names of models produced by each software package. The rightmost column presents the experimentally determined status for native chain C as part of the complex as a whole as well as its individual chains when treated as an individual unit.

Fragment	FOD	I-Tasser	Robetta	Aβ(1−40) (2MVX)
Accordant fragments (RD < 0.5)				
1−40	F1,F2,F3		R1,R2,R3,R4	
1−6	F1,F5	I1,I2,I4	R1,R2,R3,R4,R5,R6, R7,R8	Comp.
7−15	F1,F2,F3		R1,R4,R5,R6	
16−21	F1,F2,F3	I3	R1,R2,R3,R4,R6, R7,R8	Comp., Indiv.
23−28	F1,F2,F3		R1,R5,R7,R9,R10	Indiv.
29−40	F1,F2,F3		R1	
Discordant fragments (RD ≥ 0.5)				
1−40	F4,F5	I1,I2,I3,I4,I5	R5,R6,R7,R8,R9,R10	Comp., Indiv.
1−6	F2,F3,F4	I3,I5	R9,R10	Indiv.
7−15	F4,F5	I1,I2,I3,I4,I5	R2,R3,R7,R8,R9,R10	Comp., Indiv.
16−21	F4,F5	I1,I2,I4,I5	R5,R9,R10	
23−28	F4,F5	I1,I2,I3,I4,I5	R2,R3,R4,R6,R8	Comp.
29−40	F4,F5	I1,I2,I3,I4,I5	R2,R3,R4,R5,R6,R7, R8,R9,R10	Comp., Indiv.

fragments at 7−15, 16−21 and 22−27, 23−28 frequently deviate from the theoretical monocentric distribution in favor of experimentally determined properties (except for the 16−21, where such conditions are not observed).

When discussing the status of each fragment it should be noted that the evaluation criteria are supplied by the FOD model.

The 3D structures of generated models are shown in Fig. 10.B.4 (F1…F5, I1…F5, R1 … R5) and Fig. 10.B.5 (R6 … R10). Hydrophobicity profiles of selected structures accordant and discordant with the fuzzy oil drop model are shown in Fig. 10.B.6 and Fig. 10.B.7 respectively.

Analysis of results shown in Table 10.B.1 and Table 10.B.2 reveals − somewhat surprisingly − that the models produced by Robetta are largely consistent with the monocentric distribution of hydrophobicity. While the Robetta algorithm does not directly account for internalization of hydrophobic residues, it nevertheless proves that the presented chain may,

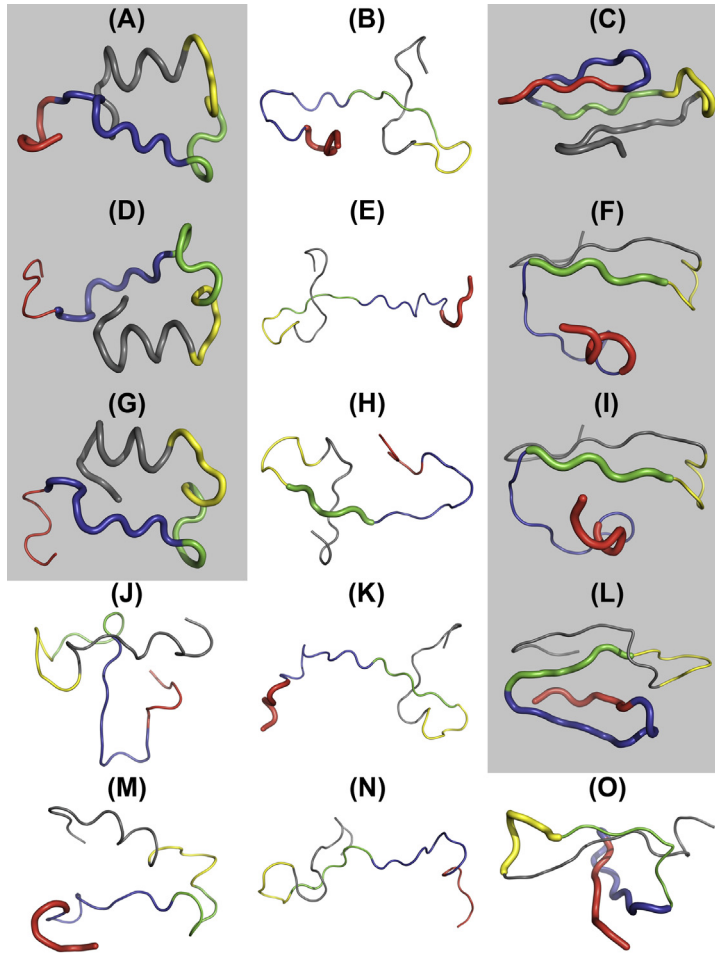

Fig. 10.B.4 3D presentation of simulated model structures of Aβ(1—40) (2MVX), part 1. A, D, G, J, M— F1…F5. B, E, H, K, N — I1—I5. C, F, I, L, O — R1 … R5. Fragments analyzed in this study are highlighted by colors: red — 1—6, blue — 7—15, green — 16—21, yellow — 23—28. Rest of each chain (29—40) is gray. Gray background denotes RD (T-O-R) < 0.5 for the whole chain (1—40). Status of each fragment of the structures is given by the backbone trace style: thick — accordant (RD < 0.5), thin — discordant (RD ≥ 0.5).

under certain circumstances, adopt a globular conformation. It is interesting to speculate why such phenomena are not observed *in vivo*.

In summary, it is worth noting that Robetta generated four models whose RD is lower than 0.5 (indicating the presence of a centralized

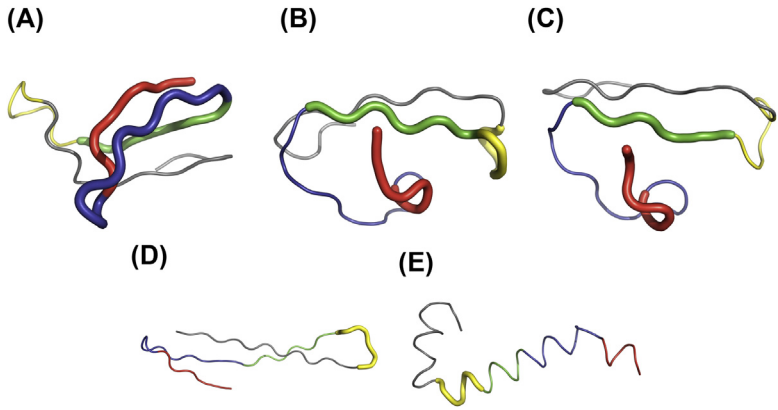

Fig. 10.B.5 3D presentation of simulated model structures of Aβ(1−40) (2MVX), part 2. A, B, C, D, E R6 … R10. Fragments analyzed in this study are highlighted by colors: red − 1−6, blue − 7−15, green − 16−21, yellow − 23−28. Rest of each chain (29−40) is gray. Gray background denotes RD (T-O-R) < 0.5 for the whole (1−40) chain. Status of each fragment of the structures is given by the backbone trace style: thick − accordant (RD $<$ 0.5), thin − discordant (RD $\geq$ 0.5).

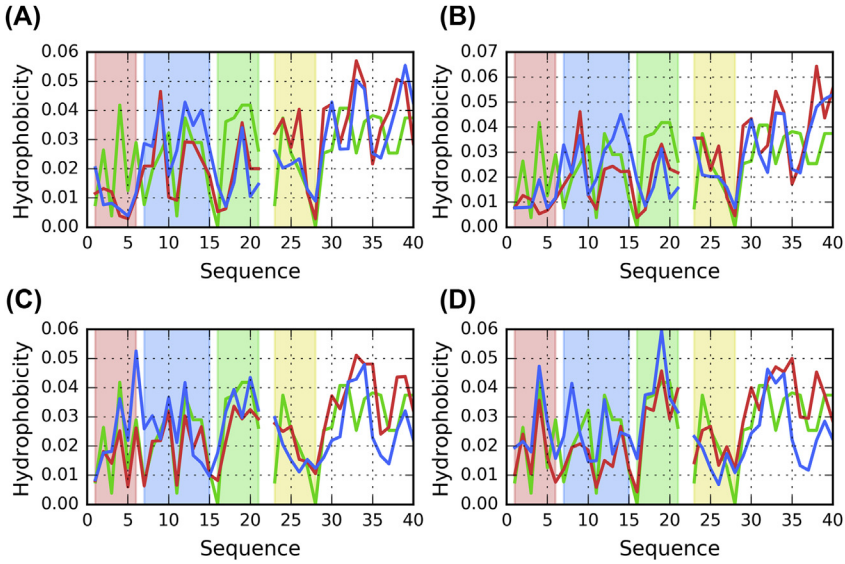

Fig. 10.B.6 Theoretical (T, blue), observed (O, red) and intrinsic (H, green) hydrophobicity distribution profiles for selected accordant simulated model structures of Aβ(1−40) (2MVX). (A) F1; (B) F2; (C) R1; (D) R2. Colored backgrounds highlight fragments analyzed in this study: red − 1−6, blue − 7−15, green − 16−21, yellow − 23−28.

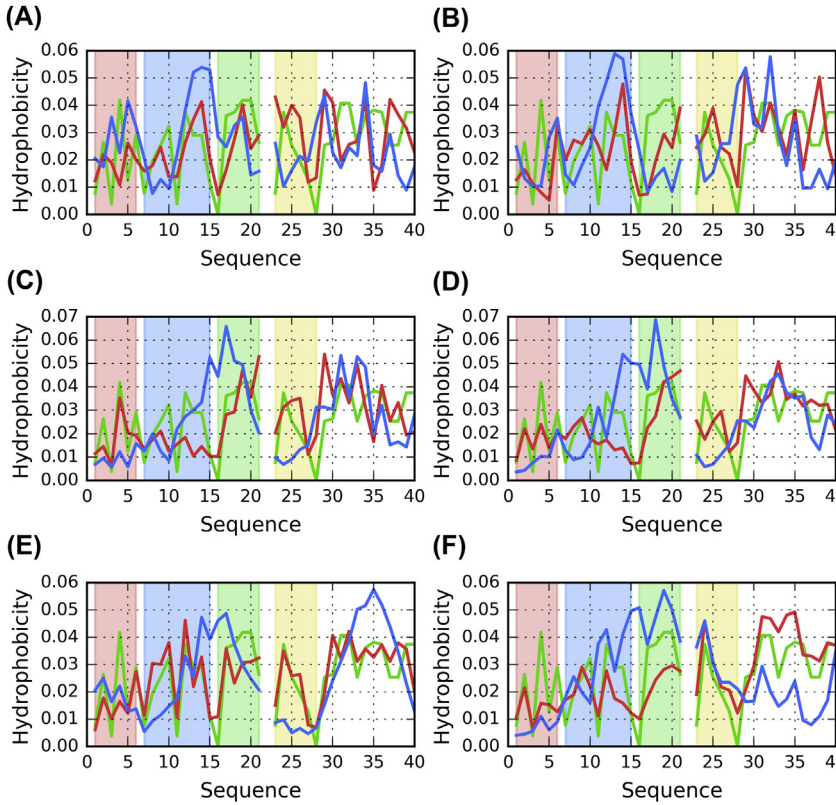

Fig. 10.B.7 Theoretical (T, blue), observed (O, red) and intrinsic (H, green) hydrophobicity distribution profiles for selected discordant simulated model structures of Aβ(1−40) (2MVX). Colored backgrounds highlight fragments analyzed in this study: red − 1−6, blue − 7−15, green − 16−21, yellow − 23−28.

hydrophobic core). In contrast, I-Tasser produced no such models. While I-Tasser models are generally more reminiscent of amyloid forms (Fig. 10.B.4), the greatest deviation from the monocentric core pattern is observed for one of the presented Robetta models. Regarding FOD, the computed models promote internalization of hydrophobic residues but are nevertheless quite divergent from globular forms [17,18].

References

[1] Schütz AK, Vagt T, Huber M, Ovchinnikova OY, Cadalbert R, Wall J, Meier BH. Atomic-resolution three-dimensional structure of amyloid β fibrils bearing the Osaka mutation. Angewandte Chemie International Edition 2014;54(1):331−5. https://doi.org/10.1002/anie.201408598.

[2] Tycko R. Molecular structure of aggregated amyloid-β: insights from solid-state nuclear magnetic resonance. Cold Spring Harbor Perspectives in Medicine 2016;6(8): a024083. https://doi.org/10.1101/cshperspect.a024083.
[3] Zhang Y. I-tasser server for protein 3D structure prediction. BMC Bioinformatics 2008;9(1):40. https://doi.org/10.1186/1471-2105-9-40.
[4] Roy A, Kucukural A, Zhang Y. I-tasser: a unified platform for automated protein structure and function prediction. Nature Protocols 2010;5(4):725−38. https://doi.org/10.1038/nprot.2010.5.
[5] Yang J, Yan R, Roy A, Xu D, Poisson J, Zhang Y. The I-tasser Suite: protein structure and function prediction. Nature Methods 2015;12(1):7−8. https://doi.org/10.1038/nmeth.3213.
[6] https://zhanglab.ccmb.med.umich.edu/I-TASSER.
[7] http://robetta.org.
[8] Kim DE, Chivian D, Baker D. Protein structure prediction and analysis using the Robetta server. Nucleic Acids Research 2004;32(Web Server):W526−31. https://doi.org/10.1093/nar/gkh468.
[9] http://predictioncenter.org.
[10] Moult J, Fidelis K, Kryshtafovych A, Schwede T, Tramontano A. Critical assessment of methods of protein structure prediction (CASP) − round x. Proteins: Structure, Function, and Bioinformatics 2013;82:1−6. https://doi.org/10.1002/prot.24452.
[11] Konieczny L, Brylinski M, Roterman I. Gauss-function-based model of hydrophobicity density in proteins. Silico Biology 2006;6(1−2):15−22.
[12] Kalinowska B, Banach M, Konieczny L, Roterman I. Application of divergence entropy to characterize the structure of the hydrophobic core in DNA interacting proteins. Entropy 2015;17(3):1477−507. https://doi.org/10.3390/e17031477.
[13] Kullback S, Leibler RA. On information and sufficiency. The Annals of Mathematical Statistics 1951;22(1):79−86. https://doi.org/10.1214/aoms/1177729694.
[14] Dułak D, Gadzała M, Banach M, Ptak M, Wiśniowski Z, Konieczny L, Roterman I. Filamentous aggregates of tau proteins fulfil standard amyloid criteria provided by the fuzzy oil drop (FOD) model. International Journal of Molecular Sciences 2018;19(10): 2910. https://doi.org/10.3390/ijms19102910.
[15] Dułak D, Banach M, Gadzała M, Konieczny L, Roterman I. Structural analysis of the Aβ(15−40) amyloid fibril based on hydrophobicity distribution. Acta Biochimica Polonica 2018. https://doi.org/10.18388/abp.2018_2647.
[16] Laskowski RA, Jabłońska J, Pravda L, Vařeková RS, Thornton JM. PDBsum: structural summaries of PDB entries. Protein Science 2017;27(1):129−34. https://doi.org/10.1002/pro.3289.
[17] Schmit JD, Ghosh K, Dill K. What drives amyloid molecules to assemble into oligomers and fibrils? Biophysical Journal 2011;100(2):450−8. https://doi.org/10.1016/j.bpj.2010.11.041.
[18] Banach M, Konieczny L, Roterman I. Fuzzy oil drop model application—from globular proteins to amyloids. Computational Methods to Study the Structure and Dynamics of Biomolecules and Biomolecular Processes 2018:639−58. https://doi.org/10.1007/978-3-319-95843-9_19.